[CONTRIBUTION FROM THE GATES AND CRELLIN LABORATORIES OF CHEMISTRY, CALIFORNIA INSTITUTE OF TECHNOLOGY, NO. 1396]

The Determination of the Structures of Complex Molecules and Ions from X-Ray Diffraction by Their Solutions: The Structures of the Groups $PtBr_6^{--}$, $PtCl_6^{--}$, $Nb_6Cl_{12}^{++}$, $Ta_6Br_{12}^{++}$, and $Ta_6Cl_{12}^{++}$

BY PHILIP A. VAUGHAN, J. H. STURDIVANT, AND LINUS PAULING

The diffraction of X-rays has been little used for determining the structure of molecules in either the gaseous or the liquid state. For a gas electron diffraction is much more successful, and for a pure liquid intermolecular scattering obscures the molecular pattern. Solute molecules, however, may in the most favorable cases be fair game: namely, the diffraction pattern obtained by passing a beam of monochromatic X-rays through a concentrated solution of a strongly scattering solute in a weakly scattering solvent consists of a series of diffuse concentric rings, the spacings and relative intensities of which depend primarily on the structure of the solute molecules; *i. e.*, the scattering function is closely approximated by that of a gas of the solute molecules. E. Rumpf[1] made use of the diffraction pattern from a solution of carbon tetrabromide in benzene to determine the Br···Br distance in this compound, and O. Kratky and W. Worthmann[2] used a similar technique to estimate the I···I distances in *p,p'*-diiododiphenylmethane and *p,p'*-diiododiphenyl ether.

We have applied X-ray diffraction from solutions to the determination of the structures of chloro- and bromoplatinic acids and some complex lower halides of niobium and tantalum. We have interpreted the diffraction photographs by the visual estimation technique which has been used in these laboratories to determine the structures of a large number of gas molecules from their electron diffraction patterns.[3] It should be noted, however, that there are significant differences between the scattering function for X-rays and that for electrons; the intensity of monochromatic X-rays scattered at angle φ from the primary beam by an almost rigid gas molecule is

$$I(\varphi) = I_e \sum_i \sum_j f_i f_j \, e^{-a_{ij}s^2} \frac{\sin sr_{ij}}{sr_{ij}}$$

where

$$I_e = I_0 \frac{e^4}{m^2c^4R^2} \frac{1 + \cos^2\varphi}{2}$$

$$s = \frac{4\pi \sin \varphi/2}{\lambda}$$

(1) E. Rumpf, *Ann. Physik*, [5] **9**, 704 (1931).

(2) O. Kratky and W. Worthmann, *Monatsh.*, **76**, 263 (1947).

(3) L. Pauling and L. O. Brockway, *J. Chem. Phys.*, **2**, 867 (1934); L. Pauling and L. O. Brockway, THIS JOURNAL, **57**, 2684 (1935); L. O. Brockway, *Rev. Mod. Phys.*, **8**, 231 (1936); V. Schomaker, Thesis, California Institute of Technology, 1938. The use of punched-card methods in carrying out the necessary calculations is discussed by P. A. Shaffer, Jr., V. Schomaker, and L. Pauling, *J. Chem. Phys.*, **14**, 659 (1946).

f_i is the atomic scattering factor for the i^{th} atom, and $e^{-a_{ij}s^2}$ is the temperature factor for the distance r_{ij}. The scattered intensity for X-rays decreases much less rapidly with angle than that for electrons, and the intensity fluctuations are not so heavily damped. The reduced intensity function,[3] which is to be compared with the visual curve, is

$$I^\circ(s) = \frac{k}{\sum_i f_i^2} \sum_i \sum_j T_{ij} \frac{f_i f_j}{r_{ij}} \sin sr_{ij}$$

where T_{ij} is an empirical factor closely related to the temperature factor of the first equation above; T_{ij} itself is often called the temperature factor. The radial distribution integral is defined in terms of $I^\circ(s)$ exactly as in the case of electron diffraction.[3]

Experimental

To use the visual method one must have photographs on which he can see enough diffraction rings to select a reasonably unique structure; moreover, these rings should be close enough together to give good contrast between maxima and minima. We have accordingly used tungsten Kα radiation and a film-to-sample distance of 5 cm. The hot-cathode, tungsten-target tube was excited at 100 kv. peak. The beam from the X-ray tube was monochromatized by reflection from the (100) face of a galena crystal, and then collimated by a cylindrical aperture 0.8 mm. in diameter and 32 mm. long. The diffracting solution in a thin-walled glass capillary of elliptical section about 0.8 mm. thick was waxed to the face of the pinhole. The distance to the flat film could be measured with an accuracy of 0.1 mm. In all photographs made with this apparatus, Eastman Kodak Co. Screen Film was used with Patterson Hi-Speed Intensifying Screens. Mostly the exposures were of the order of 1800 milliampere hours.

The effective wave length of the monochromatized beam was measured by photographing a powdered sample of galena of which the lattice constant (a = 5.92 Å.) had been measured previously with conventional diffraction apparatus. Wave length measurements were made three times during the preparation of the solution photographs to be described; the wave lengths found were 0.2109, 0.2092 and 0.2094 Å. These are all close to 0.210 Å., the average wave length of the tungsten Kα lines, and this value has been assumed in all calculations. Examination of these powder photographs also gives one an idea of the resolution obtainable with this apparatus; in general lines separated by more than 0.4 mm. (about 0.5°) were resolved.

In all of the photographs obtained with this apparatus the diffraction pattern was much more distinct on one side of the film than on the other. The phenomenon was so pronounced that all measurements and observations were made on one side, radii being measured instead of diameters. The effect can be semi-quantitatively explained by the fact that the diameter of the pinhole, the size of the monochromator, and the size of the focal spot of the X-ray tube target allow a small range of wave lengths to pass through the pinhole in such a way that diffracted rays of different wave lengths converge on one side and

diverge on the other side of the primary beam. On the side where the rays diverge the resolution is poor at all angles. On the other side the different wave lengths focus at a point which gets closer to the diffracting sample as the angle of diffraction increases. Consequently the photographic film can be placed to secure reasonably good resolution over a certain angular interval, but the resolution deteriorates at larger angles, where the rays focus close to the solution sample. This effect probably dominates in causing decrease in resolution, and accordingly largely determines the maximum angle at which useful information can be derived from the film. Observations on our diffraction photographs become somewhat unreliable at 20–22° and the limit of observation is approximately 26°.[4]

Results

Bromoplatinic Acid.—To try the method on an ion of known structure, a diffraction photograph was made of a concentrated water solution of bromoplatinic acid. The methods of interpretation and calculation to be described here were used for all the work reported in this paper. The radial distribution integral was calculated by a punched-card method[3] from the equation

$$rD(r) = \sum_{w=1}^{80} I^{\circ}(w) e^{-aw^2} \sin (0.03\, rw)$$

where $I^{\circ}(w)$ is the visual intensity function and

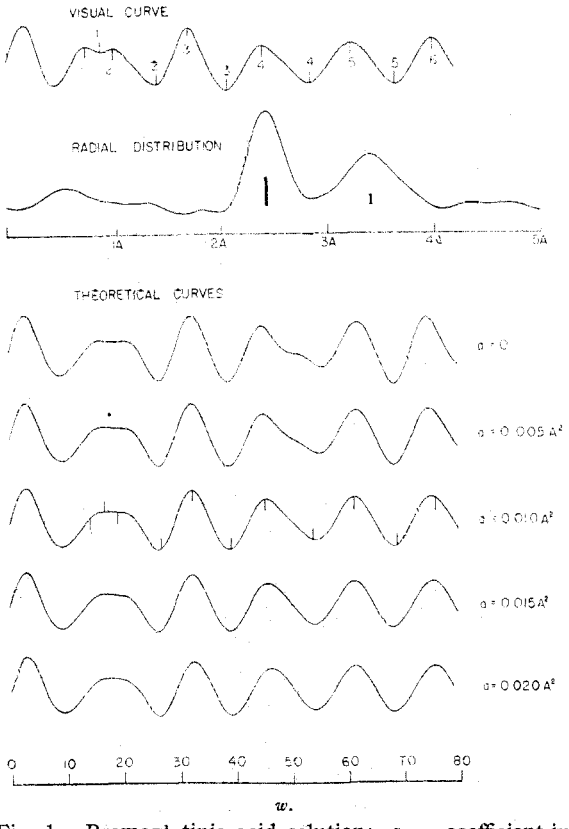

Fig. 1.—Bromoplatinic acid solution; a = coefficient in the temperature factor of the shortest Br···Br term.

(4) We contemplate the use of a curved crystal monochromator in transmission to secure symmetrical photographs of higher quality.

a is chosen so that $e^{-a(80)^2} = 0.1$. The variable w is equal to

$$\frac{70}{4\pi} s = \frac{70}{\lambda} \sin \frac{\varphi}{2} = \frac{7}{4} q$$

where q is the variable suggested by Shaffer, Schomaker, and Pauling,[3] and commonly used in electron diffraction investigations carried out at this Institute. The visual curve, radial distribution integral, and calculated curves are given in Fig. 1. Two pronounced maxima are observed on the radial distribution curve, one at 2.43 Å., and a lower, broader one at 3.41 Å. Since 3.41/2.43 = 1.403, which is very nearly $\sqrt{2}$, a regular octahedral model is clearly indicated with the Pt–Br distance equal to 2.43 Å.

In the calculation of theoretical intensity curves, the amplitudes of the Pt–Br terms were put equal to a constant, C. The Br···Br amplitudes are then given to a satisfactory degree of approximation by

$$C \frac{r(\mathrm{Pt\text{–}Br})}{r(\mathrm{Br}\cdots\mathrm{Br})} \left(\frac{f(\mathrm{Br})}{f(\mathrm{Pt})}\right)_{\text{average}}.$$

The average value of $f(\mathrm{Br})/f(\mathrm{Pt})$ over the observed angular interval is equal to 0.375.[5] The calculations were made with the equation

$$I(w) = \sum_i \sum_j \left[\sum_{k=-N}^{N} \frac{A_{ij}}{2\sqrt{\pi a_{ij}}} e^{-\frac{(k\Delta r)^2}{4a_{ij}}} \sin \frac{4\pi w}{70} (r_{ij} + k\Delta r) \right] + \sum_l \sum_m A_{lm} \sin \frac{4\pi w}{70} r_{lm}$$

where A_{ij} is the amplitude and $e^{-a_{ij}s^2}$ the temperature factor corresponding to the distance r_{ij}; the second summation includes the terms of which the temperature factors are taken to be unity. The interval Δr was chosen as 0.087 Å. The number N was chosen to make negligibly small the factor

$$\frac{A_{ij}}{2\sqrt{\pi a_{ij}}} e^{-\frac{[(N+1)\Delta r]^2}{4a_{ij}}}$$

In Fig. 1 theoretical curves are given with $a_{\mathrm{Br}\ldots\mathrm{Br}}$, the coefficient in the exponent of the temperature factor of the Br···Br terms, equal to 0, 0.005, 0.010, 0.015 and 0.020 Å.^{2} respectively. With no temperature factor there is a pronounced shoulder on the outside of the fourth maximum instead of the asymmetry which is indicated by the visual curve; the fourth minimum is also farther to the right than observed, and the separation of the fourth and fifth maxima is too great. The curve with $a_{\mathrm{Br}\ldots\mathrm{Br}}$ equal to 0.010 Å.^{2} gives good agreement with the visual intensity curve with the exception of the first and second maxima. Since the first peak on the theoretical curve might well give the appearance of a doublet as indicated on the visual curve, the principal disagreements are in the measurements. It will be remembered, however, that if intermolecular

(5) "Internationale Tabellen zur Bestimmung von Kristallstrukturen," Vol. II, reprinted by Edwards Bros., Ann Arbor, Michigan, 1944, p. 572.

TABLE I[a]

a In this and all similar tables the scale of the theoretical curve has been adjusted to make the average value of $w_{calcd.}/w_{obsd.}$ for the most reliably measured features equal to 1.000.

Feature Max.	Min.	$w_{obsd.}$	$w_{calcd.}/w_{obsd.}$ $a_{Br\cdots Br} = 0.010$ Å.^{2}
1		14.2	(1.162)
	1	16.8	(1.102)
2		19.9	(1.056)
	2	27.0	(0.981)
3		32.6	.997
	3	39.5	.992
4		45.7	1.002
	4	54.3	1.006
5		61.6	0.997
	5	69.3	(.988)
6		76.2	(.987)
Average deviation (5 features)			.004

terms affect the curve at all, they do so near the first maximum. Moreover, on practically all of the photographs examined the first maximum has been measured too close to the center of the film. Table I gives a comparison of the maxima and minima observed on the film and the theoretical curve with $a_{Br\cdots Br}$ equal to 0.010 Å.^{2}. For each curve, the most probable Pt–Br distance is 2.43 Å.; this agrees well with the sum of the radii, which is 2.45 Å.[6]

Chloroplatinic Acid.—One of the authors had obtained two diffraction photographs of a saturated aqueous solution of chloroplatinic acid nine years before the other work described herein was begun. From these photographs the structure of the chloroplatinate ion has been determined. The radiation was nominally tungsten Kα, selected by monochromatization as in the later experiments. There is no check on the effective wave length, however, and the film distance was not determined with a high degree of precision; hence the accuracy of the scale factor is unknown. Nevertheless, the observed data are in accord with the octahedral model and are therefore presented as a verification of the solution method.

The visual curve, radial distribution integral, and theoretical curves are given in Fig. 2. The radial distribution integral has a very prominent maximum at 2.37 Å., and a smaller one at 3.35 Å., in accord with the octahedral model. The principal characteristics of the calculated scattering functions are observable on the visual curve; the breadth of the first maximum, the sharpness of the second, the asymmetry of the third, and the separation of the second and third maxima by a smaller interval than the third and fourth. The curves with $a_{Cl\cdots Cl}$ equal to 0.005 and 0.010 Å.^{2} agree best with the visual curve.

Table II compares the observed and calculated positions of the maxima and minima. The Pt–Cl distance obtained (unreliable for reasons given above) is 2.39 Å. This agrees poorly with the sum of the octahedral radii, which is 2.30 Å.[5] The Pt–Cl distance in K_2PtCl_6 is reported to be 2.33 Å.[7]

TABLE II

Feature Max.	Min.	$w_{obsd.}$	$w_{calcd.}/w_{obsd.}$ $a_{Cl\cdots Cl} = 0.010$ Å.^{2}
1		19.1	(0.954)
	1	27.8	(0.950)
2		33.2	0.997
	2	39.8	1.008
3		46.7	1.010
	3	54.9	1.007
4		63.0	0.993
	4	71.0	0.984
5		78.4	(0.982)
	Average deviation		0.008

gam to obtain a lower chloride to which he assigned the formula $TaCl_2 \cdot 2H_2O$. The compound is somewhat soluble in water, forming a dark green solution from which it can be crystallized in small hexagonal crystals. Other workers have since prepared this compound and the analogous bromide and a number of their derivatives. Formulas which have been suggested are $Ta_6Cl_{14} \cdot 7H_2O$,[9] $HTa_3Cl_7 \cdot 4H_2O$,[10] and $Ta_3Cl_7O \cdot 3H_2O$.[11]

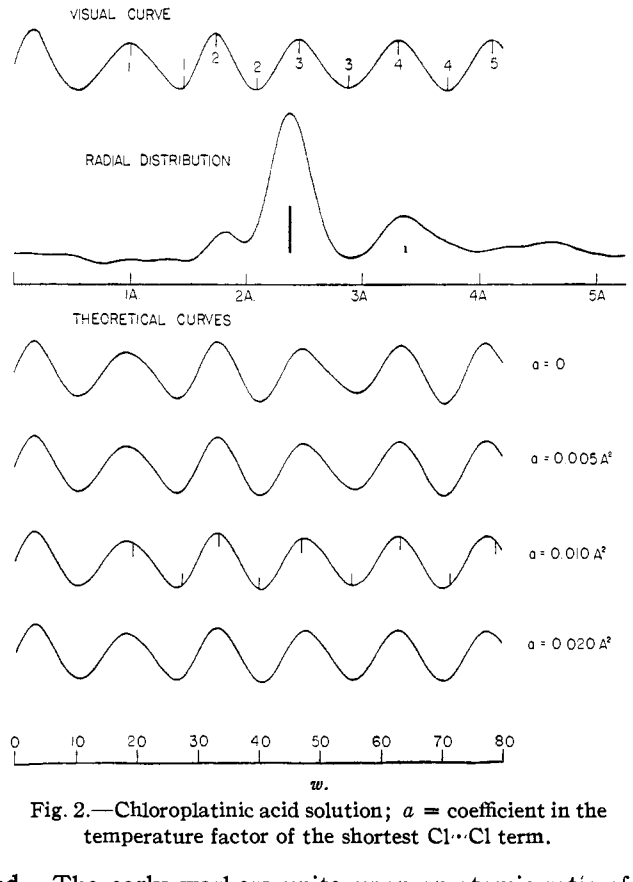

Fig. 2.—Chloroplatinic acid solution; a = coefficient in the temperature factor of the shortest Cl··Cl term.

Lower Halide Complexes of Niobium and Tantalum: Chemistry.—In 1907 Chabrié[8] reduced tantalum pentachloride with sodium amal-

The early workers unite upon an atomic ratio of halogen to tantalum equal to 7/3, but obviously disagree as to the oxidation number of tantalum.

(6) L. Pauling, "Nature of the Chemical Bond," Cornell University Press, Ithaca, New York, 1940, pp. 164 and 182.

(7) F. J. Ewing and L. Pauling, *Z. Krist.*, **68**, 223 (1928).

(8) M. C. Chabrié, *Compt. rend.*, **144**, 804 (1907).

(9) W. H. Chapin, THIS JOURNAL, **32**, 327 (1910).

(10) K. Lindner and H. Feit, *Z. anorg. allgem. Chem.*, **137**, 66 (1924).

(11) O. R. Ruff and H. Thomas, *ibid.*, **148**, 1 and 19 (1925).

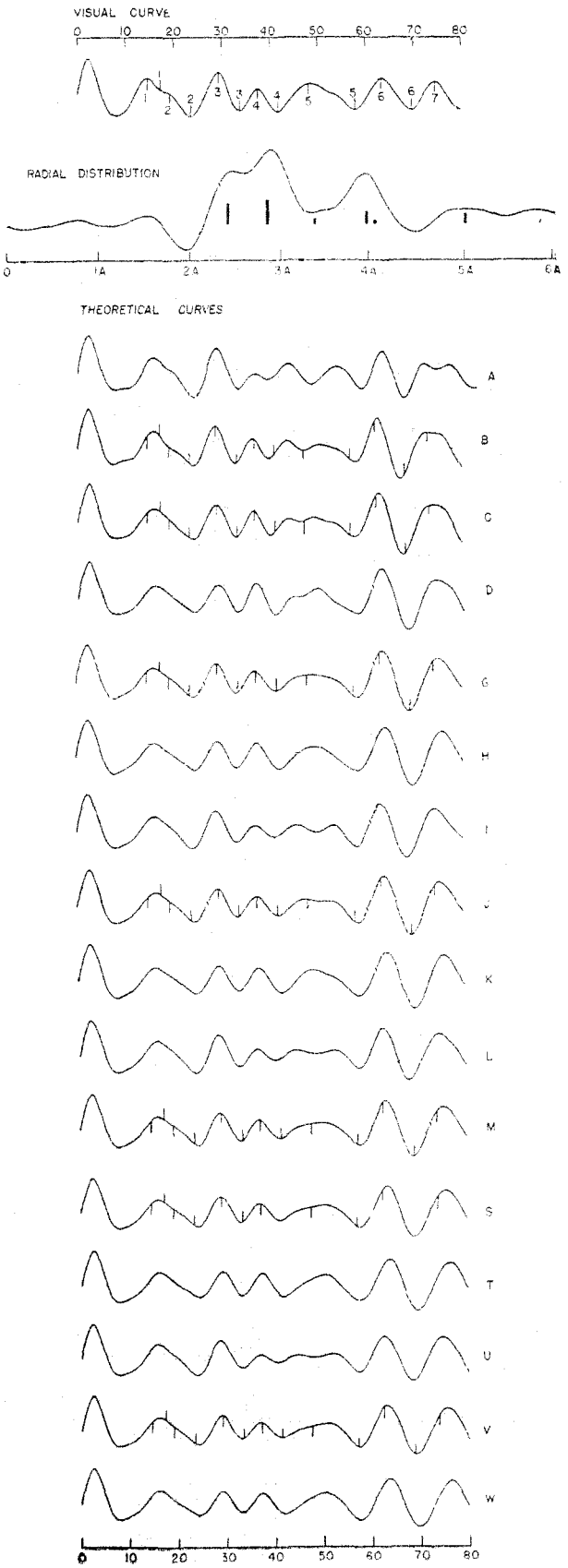

Fig. 3.—$Nb_6Cl_{14}\cdot 7H_2O$ dissolved in ethanol.

Chapin[9] measured the molecular weight by the boiling point method in propyl alcohol solution, and showed that the molecules present in this solvent contain six tantalum atoms. The second and third formulas, which were not based on a molecular weight determination, would then be rewritten $H_2Ta_6Cl_{14}\cdot 8H_2O$ and $Ta_6Cl_{14}O_2\cdot 6H_2O$; they correspond to tantalum oxidation numbers of +2 and +3, respectively. A fact of considerable import is that two of the fourteen halogen atoms ionize in aqueous solution and are readily replaced by other groups. Thus the part of the molecule most pertinent to its structure is the (Ta_6X_{12}) group, and it is with this group that the following investigations are concerned. For convenience we shall write the formulas for these complex compounds as $Ta_6X_{14}\cdot 7H_2O$, although we do not wish to imply any preference for an oxidation number of +2 1/3.

H. S. Harned[12] prepared a compound which his analyses indicated to be $Nb_6Cl_{14}\cdot 7H_2O$; he also showed by potentiometric titration with silver nitrate solution that two of the fourteen chlorine atoms are easily removed. Therefore this compound seems to be analogous to $Ta_6Cl_{14}\cdot 7H_2O$ and $Ta_6Br_{14}\cdot 7H_2O$.

Professor Harned was kind enough to lend us a considerable quantity of his chloroniobium compound which was used for the structure determination described herein. We attempted to synthesize the bromoniobium compound by reduction of niobium pentabromide. Both granulated lead and sodium amalgam were tried as reducing agents, but in neither case was a significant quantity of the desired compound obtained.

The bromo- and chlorotantalum complexes were prepared by reduction of the corresponding pentahalide with granulated lead in a nitrogen atmosphere at red heat, as described by Lindner and Feit.[10] The compound was extracted from the resulting mass with dilute aqueous hydrogen halide.

None of the complex compounds described above is soluble enough in water to give satisfactory aqueous solution photographs. All, however, are extremely soluble in ethanol, and this solvent was used exclusively. Since these compounds are presumably not ionized in ethanol solution, the principal diffracting molecules contain fourteen halogen and six tantalum atoms.

The Structure of the Nb_6Cl_{12} Group.—Four diffraction photographs were made of concentrated alcoholic solution of $Nb_6Cl_{14}\cdot 7H_2O$. The visual curve and radial distribution integral are given in Fig. 3.

(12) H. S. Harned, THIS JOURNAL, **35**, 1078 (1913).

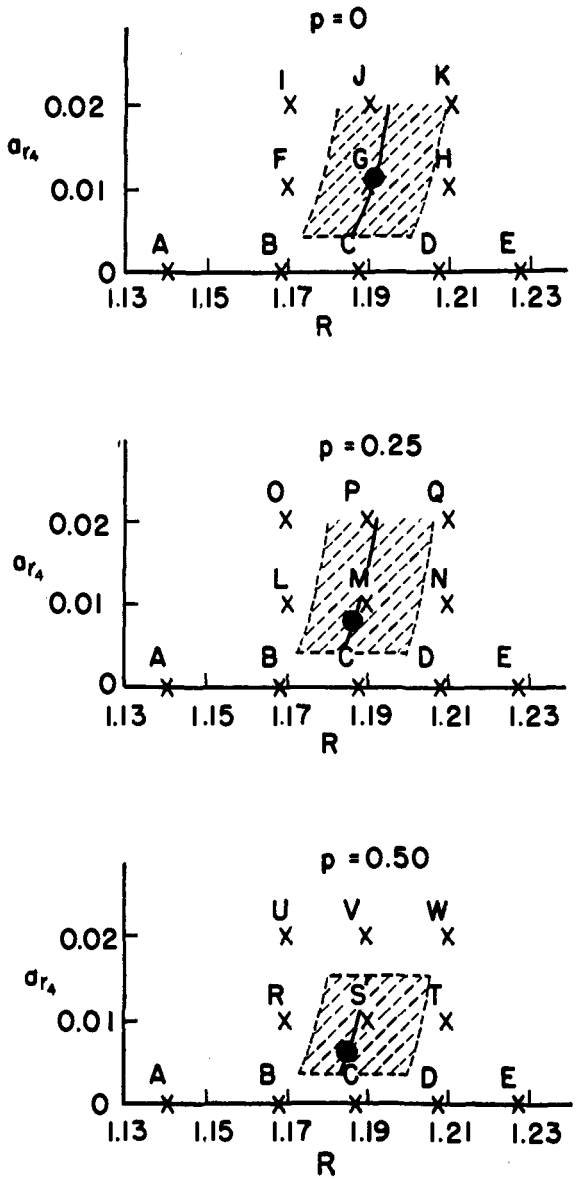

Fig. 4.—Parameters of models used to calculate scattering curves for the Nb_6Cl_{12} group; R = ratio of Nb–Nb to Nb–Cl distance; a_{r_4} is the coefficient in the temperature factor of r_4, $p = a_{r_3}/a_{r_4}$; the shaded area is the region of acceptability.

The radial distribution function has two incompletely resolved peaks in the vicinity of 2.4 and 2.9 Å., the latter being considerably the higher. There are also a prominent peak at 3.95 Å. and a rather low one at approximately 5 Å. The trial structure must be chosen consistent with the chemistry of the compounds and with the radial distribution curve. From chemical considerations two of the chlorine atoms are not related by symmetry to the other twelve. A structure which suggests itself is the following: Place the six niobium atoms at the corners of a regular octahedron whose edges are 2.9 Å. long. Then place

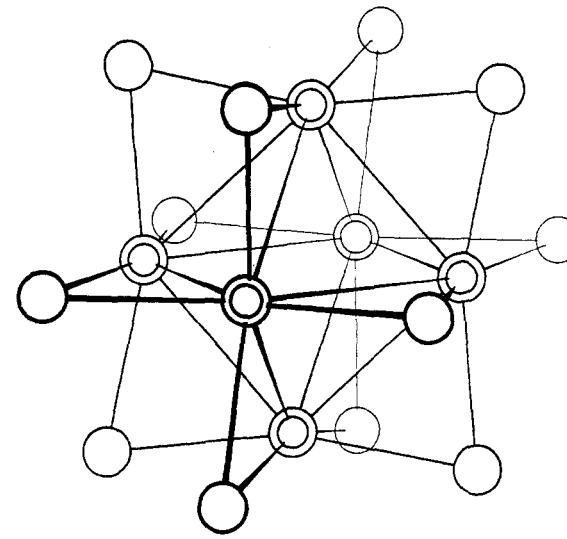

Fig. 5.—Structure of the Nb_6Cl_{12}, Ta_6Br_{12}, and Ta_6Cl_{12} groups; double circles are metal atoms, single circles are halogen atoms.

twelve chlorine atoms on the radial perpendicular bisectors of the edges so that the shortest niobium–chlorine distances are approximately 2.4 Å. (see Fig. 5). The most prominent distances are as follows:

Designation	Description
r_1	Twelve Nb–Nb distances at 2.9 Å.
r_2	Twenty-four Nb–Cl distances at 2.4 Å.
r_3	Twenty-four Nb · · · Cl distances at 3.95 Å.
r_4	Twenty-four Nb · · · Cl distances at 5.0 Å.

This structure meets all of the requirements of the known chemistry of the molecule and the radial distribution function. No attempt has been made to locate the two remaining chlorine atoms, since their direct effect on the intensity function will be small. They may perhaps however cause significant distortion from the symmetrical structure.

The assumption of cubic symmetry leaves only two parameters to be determined, a scale parameter and the ratio (r_1/r_2) of the shortest Nb–Nb to the Nb–Cl bonded distance. The following theoretical curves were calculated and are shown in Fig. 3.

Designation	$(r_1/r_2) = R$
A	1.137
B	1.168
C	1.187
D	1.207
E	1.227

These curves were calculated with $(f_{Cl}/f_{Ta})_{average} = 0.348$.[5]

Curve C gives the best agreement with the visual curve. There are, however, certain objections to all of these curves. In curve B the fourth minimum is not so wide and deep as the

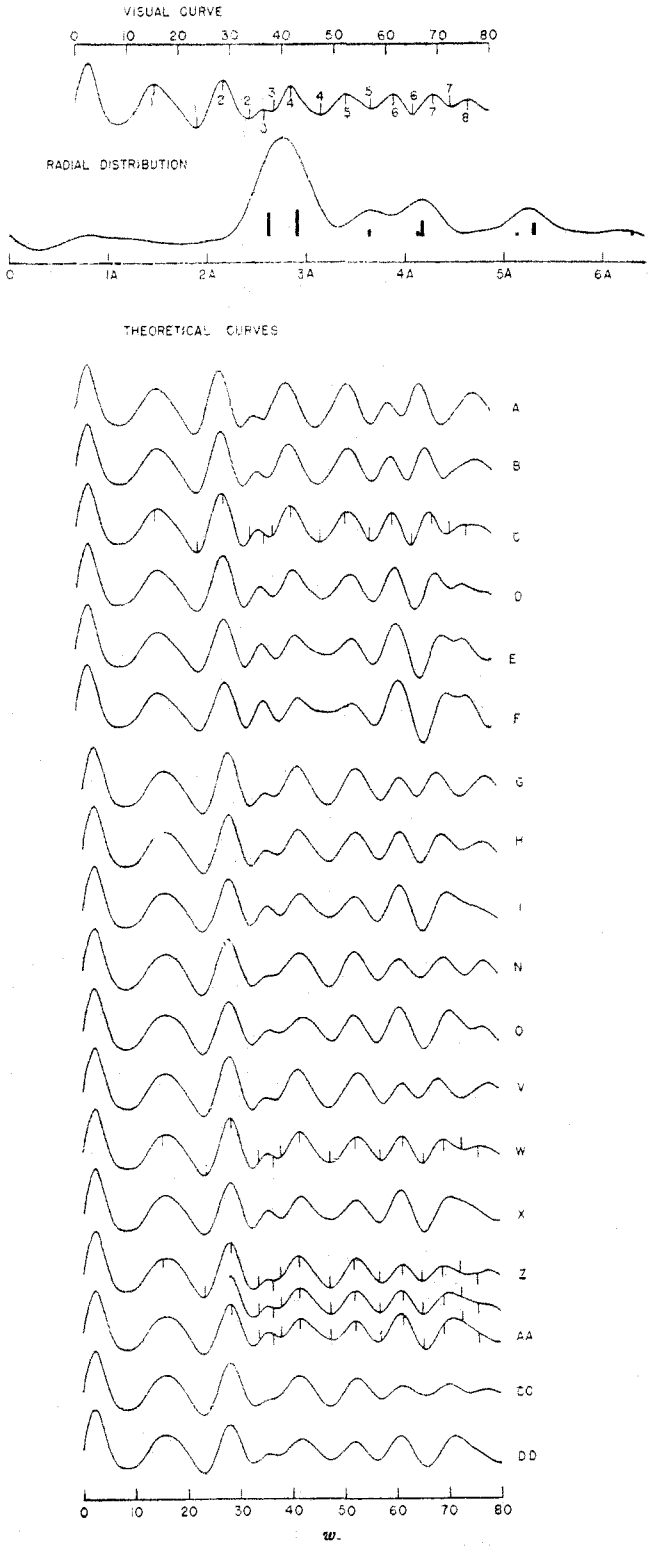

Fig. 6.—$Ta_6Br_{14}\cdot 7H_2O$ dissolved in ethanol.

film suggests. Moreover, the broad feature which we have identified with the fifth maximum contains a minimum which one might expect to see. These discrepancies seem to be at least partially corrected by increasing R slightly, as in curve C, but then the fourth maximum becomes more prominent than it should be; this maximum appears on the film to be considerably lower than the average of the third and fifth maxima. The radial distribution curve points to the remedy; the width of the peak at 5 Å. indicates that a temperature factor must be applied to r_4. Since it is not likely that a_{r_4} will be fairly large and a_{r_3} zero, it becomes necessary to investigate the effect of a temperature factor on both long Nb···Cl distances. A number of theoretical curves were calculated in which both of these temperature factors were varied; a selection are shown in Fig. 3. No temperature factors were applied to the long Nb···Nb distance or to the Cl···Cl distances, since these terms contribute but little to the scattering curve. The two least important Cl···Cl terms were omitted completely. The parameters used to calculate each of the curves can be found by reference to Fig. 4, in which the parameters of each curve are shown graphically. The shaded area represents the region of acceptability. The full, curved line in each diagram is the locus of the best values of R. The large dot marks the best parameters for each value of the temperature-factor ratio.

The theoretical curves in Fig. 3 show that the temperature factor on the longest Nb···Cl distance helps considerably, even if a_{r_4} is as small as 0.005 Å.^{2} Too large a value of a_{r_3}, however, makes the fourth minimum too shallow and affects adversely the shape of the broad fifth maximum; the most that can be allowed is about 0.005 Å.^{2} Values of a_{r_4} from 0.005 to 0.010 Å.^{2} and of a_{r_3} from zero to 0.005 Å.^{2} produce satisfactory agreement with the visual curve and are consistent also with the results on bromoplatinic acid. There are at least three possible explanations for the temperature factors: (1) the presence of considerable thermal motion; (2) small splitting of the distances due to distortions introduced by the two replaceable chlorine atoms; and (3) decrease of resolution due to the experimental arrangement.

Fortunately the choice of the best value of R and the scale factor varies but little with the temperature factors assigned to the longer distances. A comparison of the observed and calculated positions of the maxima and minima will be found in Table III. We have concluded that the best choice of parameters is 2.85 Å. for the shortest Nb–Nb distance and 2.41 Å. for the shortest Nb···Cl distance.

The four principal sources of error are (1)

TABLE III

Feature Max.	Min.	$w_{obsd.}$	$w_{calcd.}/w_{obsd.}$ B	C	M	S
1		14.7	(1.096)	(1.099)	(1.105)	(1.110)
	1	17.4	...	...	...	...
2		19.3	...	...	...	...
	2	23.7	(1.050)	(1.032)	(1.035)	(1.035)
3		29.4	1.000	1.000	0.995	1.000
	3	33.8	0.995	0.998	.989	.990
4		37.6	.992	.994	.994	.998
	4	41.9	.977	.981	.997	.995
5		48.2	...	...	...	...
	5	57.9	1.025	1.013	1.009	1.000
6		63.3	1.012	1.012	1.009	1.014
	6	69.7	(0.990)	(0.994)	(0.996)	(1.002)
7		74.6	(1.012)	(1.015)	(1.019)	(1.027)
Average deviation (6 features)			0.012	0.009	0.007	0.005
Parameters, Å. Shortest Nb–Nb			2.84	2.85	2.86	2.84
Shortest Nb···Cl			2.44	2.40	2.40	2.39

qualitative errors in drawing the observed intensity curve, (2) errors in measuring the radii of the rings, (3) possible errors in the mean wave length, and (4) spectral impurity of the monochromatized beam, which might distort the photograph. The limit of error due to the first two sources is estimated from the region of acceptability in Fig. 4 and from the average deviations in Table III to be approximately ±0.05 Å. for r_1 and r_2. A reasonable estimate of the total limit of error is 0.07 Å.

The Structure of the Ta_6Br_{12} Group.—The visual curve and radial distribution integral for a solution of $Ta_6Br_{14}\cdot 7H_2O$ in ethanol solution are shown in Fig. 6. In the latter curve there is a very high, broad maximum at 2.72 Å. and smaller maxima at 3.64, 4.16, and 5.25 Å. The similarity to the radial distribution function for $Nb_6Cl_{12}\cdot 7H_2O$ is immediately apparent, but all of the metal–halogen distances are longer because of the larger radius of bromine. The shortest Ta–Ta and Ta–Br distances are so close together that they are unresolved. The same model was assumed as for the Nb_6Cl_{12} group (Fig. 5). The theoretical curves shown in Fig. 6 were calculated for the models identified below.

Designation	$(r_1/r_2) = R$
A	1.066
B	1.082
C	1.098
D	1.114
E	1.132
F	1.150

The average value of the ratio of the scattering factor of bromine to that of tantalum was taken as 0.40.[5] Although the position and shape of the low third maximum are very difficult to determine, it is certain that this peak is very much lower than the fourth maximum and that the second minimum is considerably deeper than the third, which possibly may not even be a real minimum. The fourth maximum is higher than the fifth, while the fifth, sixth and seventh maxima are of approximately equal height. However, some disagreement with the last observation must not be considered important. The sixth minimum is definitely deeper than the fifth. It is extremely difficult to see the eighth maximum, and since it occurs quite far out on the film one cannot even be sure that it is present.

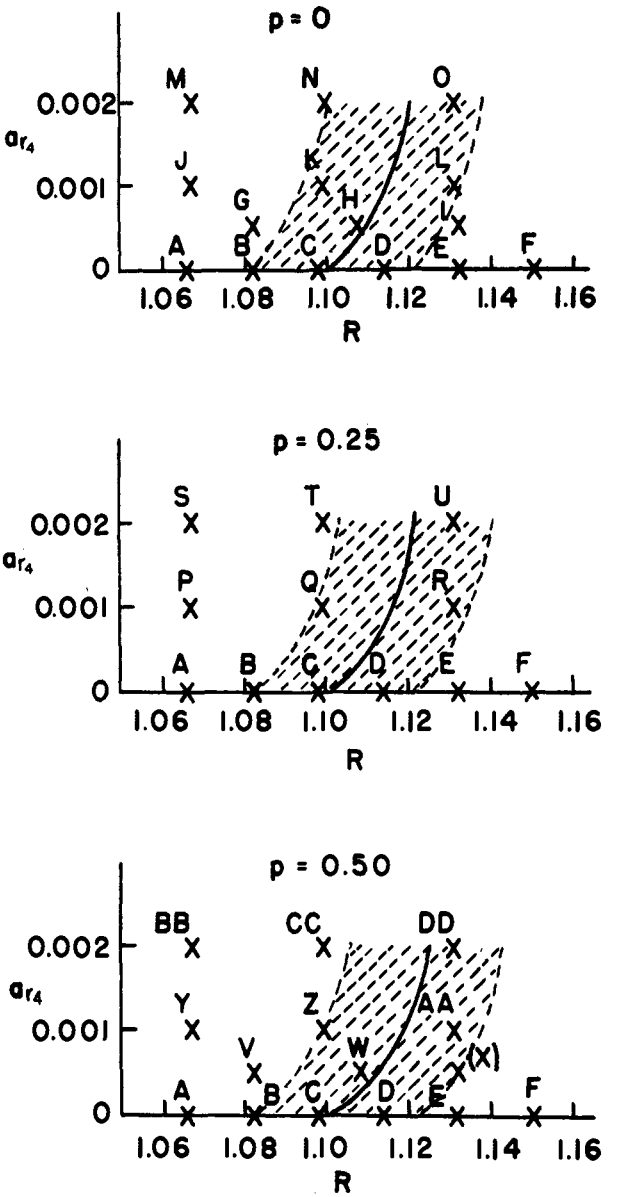

Fig. 7.—Parameters of models used to calculate scattering curves for the Ta_6Br_{12} group; R = ratio of Ta–Ta to Ta–Br distance; a_{r_4} is the coefficient in the temperature factor of r_4; $p = a_{r_3}/a_{r_4}$; the shaded area is the region of acceptability.

Model C gives the best agreement with the

TABLE IV

Feature Max.	Min.	$w_{obsd.}$	$w_{calcd.}/w_{obsd.}$ C	W	Z	AA
1		15.2	(1.039)	(1.044)	(1.073)	(1.051)
	1	23.5	(0.996)	(0.986)	(0.982)	(0.978)
2		28.4	.993	.997	.992	.988
	2	33.6	(.964)	(.960)	(.973)	(.960)
3		36.4	(.970)	(.971)	(.977)	(.974)
	3	37.9	(.986)	(.985)	(.979)	(.994)
4		41.5	1.000	.999	.995	1.001
	4	47.3	0.996	1.001	1.005	1.007
5		52.1	1.015	1.010	1.009	0.999
	5	56.9	1.009	1.004	1.008	.987
6		61.3	1.002	0.997	1.001	.991
	6	65.1	0.997	0.997	1.001	1.007
7		69.0	0.991	1.002	1.004	1.023
	7	72.4	(0.993)	(1.011)	...	...
8		75.7	...	(1.007)	...	...
Average deviation (8 features)			0.006	0.003	0.005	0.009
Parameters, Å., Shortest Ta–Ta			2.90	2.91	2.89	2.94
Shortest Ta–Br			2.64	2.63	2.63	2.60

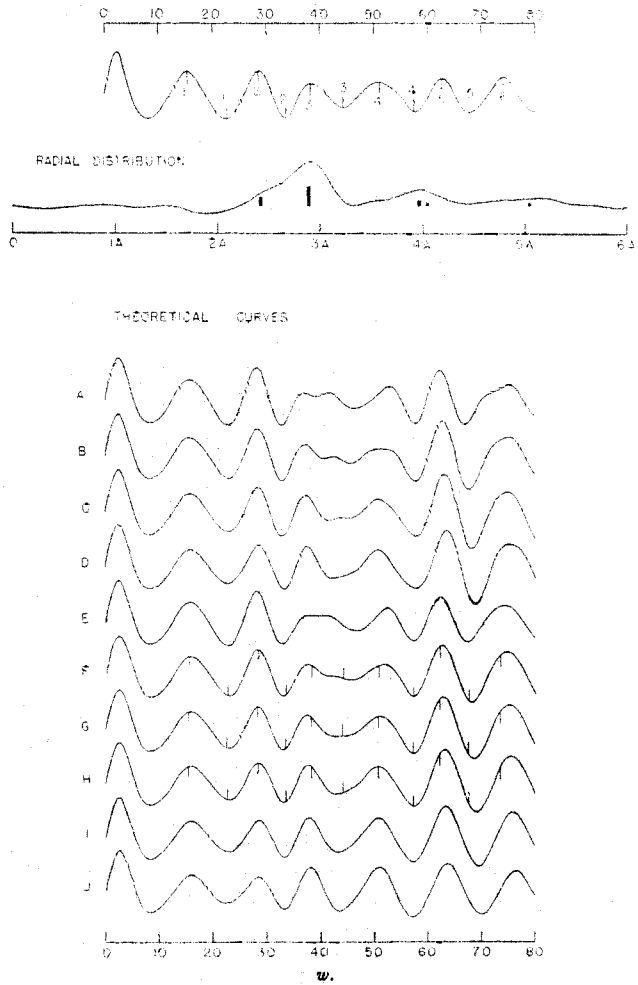

Fig. 8.—$Ta_6Cl_{14}\cdot 7H_2O$ dissolved in ethanol.

visual curve. Model E cannot be accepted because of the heights of the third and sixth maxima and the depth of the third minimum. Model D, however, is acceptable. Model B gives poor agreement and represents the approximate limit of acceptability in this direction. In this curve the fifth maximum is too high and the sixth minimum too shallow compared to the fifth. Table IV gives the observed and calculated (Model C) positions of the maxima and minima. A slight increase in R over that of Model C seems desirable, and the best parameters are 2.90 Å. for the Ta–Ta and 2.63 Å. for the Ta–Br distances.

In spite of the satisfactory agreement between observed and calculated intensity curves, we cannot be content with the above determination. For the chloroniobium and the bromoplatinate ions the best agreement was obtained when temperature factors were applied to the longer distances. We should therefore investigate the effect of such temperature factors on the theoretical intensity curves of the bromotantalum ion. Theoretical curves were calculated in which the longest (r_4) and next longest (r_3) Ta···Br distances were assigned various temperature factors; some of these curves are shown in Fig. 6. The various parameters of each curve are shown graphically in Fig. 7. Each Br···Br distance was assigned the same temperature factor as the Ta···Br distance nearest it in length. Satisfactory curves could be obtained for any of the temperature factors considered. However, those curves for which the ratio p is 1/2 are preferred because the relative heights of the fourth and fifth maxima are in better agreement with the visual curve. The heavy full lines in Fig. 7 represent the loci of the optimum values of R and the shaded area is the region of acceptability. The most satisfactory value of R increases considerably as a_{r_4} increases, but does not vary appreciably with p, in the range considered. Examination of the theoretical curves does not enable one to choose optimum values for the temperature factors and hence decide on the most satisfactory value of R. However, previous experience has shown that values of a_{r_4} in the range 0.005 to 0.01 Å.[2] for the longest Ta···Br distance are most reasonable. Therefore we choose the following parameters and limits of error: shortest Ta–Ta distance, 2.92 ± 0.07 Å.; shortest Ta–Br distance, 2.62 ± 0.07 Å.

The Structure of the Ta_6Cl_{12} Group.—The visual intensity curve and the radial distribution function calculated therefrom are shown in Fig. 8. The latter curve is consistent with the structure proposed for the Nb_6Cl_{12} and Ta_6Br_{12} groups. The large maximum at 2.9 Å. is the shortest Ta–Ta distance, and the decided asymmetry on the inside of this peak corresponds to the shortest Ta–Cl

distance. The prominent maximum around 4.0 Å. and the very low one near 5 Å. correspond to longer Ta···Cl and Ta···Ta terms and occur at the expected positions. In order to find the ratio (r_1/r_2) of the shortest Ta–Ta to the shortest Ta–Cl distance, theoretical curves were calculated for the following models:

Designation	R	a_{r_4}, Å.²	a_{r_3}, Å.²
A	1.137	0	0
B	1.169	0	0
C	1.188	0	0
D	1.208	0	0
E	1.137	0.010	0.005
F	1.169	.010	.005
G	1.188	.010	.005
H	1.208	.010	.005
I	1.228	.010	.005
J	1.256	.010	.005

These theoretical curves are also shown in Fig. 8. A value of 0.19 was used for the average ratio of the scattering factor of chlorine to that of tantalum.[5]

Theoretical curves were not calculated using temperature factors other than those given above, since these had been found satisfactory for the Nb_6Cl_{12} and Ta_6Br_{12} structure determinations. Moreover, the metal–halogen terms are much less important in this case than in the others. It will be noticed, however, that better agreement with the visual curve is obtained when temperature factors are used. Model G gives the best agreement, and the optimum value with limit of error of R is 1.18 ± 0.04. For smaller values of R, as in Model E, the shape of the third maximum and the position of the third minimum disagree seriously with the observations. At larger values of R, the third maximum becomes too high, the third minimum too deep, and errors in the positions of the maxima and minima increase. A comparison between the observed and calculated positions of the maxima and minima is presented in Table V for Models F and G. The optimum parameters and limits of error are 2.88 ± 0.05 Å. for Ta–Ta and 2.44 ± 0.10 Å. for Ta–Cl.

TABLE V

Feature Max.	Feature Min.	$w_{obsd.}$	$w_{calcd.}/w_{obsd.}$ F	G
1		15.4	(1.033)	(1.039)
	1	22.7	(1.016)	(1.016)
2		28.4	1.000	1.003
	2	33.6	0.986	0.989
3		38.4	0.981	0.983
	3	44.4	(1.032)	(0.993)
4		51.1	1.019	1.005
	4	57.6	1.000	1.002
5		62.6	1.007	1.010
	5	68.0	1.008	1.016
6		74.0	(1.018)	(1.023)
Average deviation (7 features)			0.010	0.009
Parameters, Å.				
Shortest Ta–Ta			2.88	2.88
Shortest Ta–Cl			2.46	2.42

Discussion

A summary of the interatomic distances in the halide complexes of niobium and tantalum which have been investigated is given below. Important distances[13] are also given for a somewhat similar complex of molybdenum. In the molybdenum compound the metal atoms are again at or near the vertices of a regular octahedron; the eight halogen atoms, however, lie at the vertices of a circumscribed cube. Bonds are also formed with oxygen atoms at the vertices of a larger octahedron.

Compound	Shortest M–M, Å.	Shortest M–X, Å.	Shortest X···X, Å.	½ (M–M), Å.
$Nb_6Cl_{14}\cdot 7H_2O$	2.85	2.41	3.37	1.425
$Ta_6Cl_{14}\cdot 7H_2O$	2.88	2.44	3.41	1.44
$Ta_6Br_{14}\cdot 7H_2O$	2.92	2.62	3.64	1.46
$Mo_6Cl_8(OH)_4\cdot 14H_2O$	2.63 (av.)	2.56 (av.)		1.315

The deviation of the intermetallic distances of tantalum and niobium in these compounds from their average value (2.88 Å.) is within the limits of error of this determination and may not be real.

Metal–metal bonds are present in all of these compounds. It is of interest to investigate the prediction which can be made from Pauling's[14] equation

$$R(1) - R(n) = 0.30 \log n$$

which gives the difference in radius between bonds of bond numbers one and n. In this case $n = v/12$ where v is the number of electron pairs forming the twelve bonds in the Ta_6 (or Cb_6 or Mo_6) grouping. The single bond radii $R(1)$ are given in Pauling's paper; they were calculated from the structures of the pure metals using this same equation. If we assume that the valence electrons of the halide ions make no contributions to the metallic bonds, then $v = 3(5 - u)$ for niobium and tantalum, where u is the oxidation number. The oxidation numbers that correspond to the three suggested formulas are +3, $+2^1/_3$, and +2. The predicted metallic radii for tantalum complexes are

Oxidation number	Bond number	Predicted radii, Å.
+3	0.5	1.433
$+2^1/_3$	.67	1.395
+2	.75	1.380

The corresponding radii for niobium are not significantly different. The experimentally determined radii are close enough to these values to be reasonable. If the equation is used to determine the bond numbers, the results are 0.41 for $Ta_6Br_{14}\cdot 7H_2O$, 0.47 for $Ta_6Cl_{14}7H_2O$, and 0.53 for $Nb_6Cl_{14}\cdot 7H_2O$. It is not to be implied that these results favor one of the proposed oxidation states for

(13) Cyrill Brosset, *Arkiv för Kemi, Mineralogi och Geologi*, **A20** (1945) and **A22** (1946).

(14) L. Pauling THIS JOURNAL, **69**, 542 (1947).

tantalum and niobium; the equation is not sufficiently reliable for such a prediction, and the effect of the halogen atoms might well be far from negligible. The predicted molybdenum radius in the $(Mo_6Cl_8)^{++++}$ group is 1.296 Å. if we assume four metallic valence electrons per molybdenum atom.

The shortest interhalogen distances in the tantalum and niobium complexes are somewhat shorter than twice the corresponding van der Waals radii (1.80 for chlorine and 1.95 for bromine). This is not unusual, however, where the halogens are in the same molecule and particularly where they are bound to the same atom.

Subtraction of the halogen radius[6] from the corresponding metal–halogen distance gives a value for the metallic radius very nearly equal to one-half the intermetallic distance. This observation indicates that the bonds are covalent and of reasonable lengths. Subtraction of the ionic halogen radii from the corresponding distances gives unreasonably small values for the effective metallic radii. The covalent nature of the bonds is, of course, indicated by the stability of the Ta_6Cl_{12} group.

Acknowledgment.—The authors are grateful to Professor Verner Schomaker for advice concerning the interpretation of the photographs.

Summary

A solution of a strongly scattering solute in a weakly scattering solvent yields an X-ray diffraction pattern which closely approximates the diffraction pattern from a gas of the solute molecules. The visual estimation method has been applied to analyze the diffraction patterns from several solutions, and the structures of several complex molecules have thereby been determined.

Suitable photographs were obtained with tungsten $K\alpha$ radiation monochromatized by crystal reflection.

For aqueous chloroplatinic and bromoplatinic acids the diffraction data correspond to an octahedral PtX_6 group.

Diffraction patterns from ethanol solutions of $Nb_6Cl_{14}\cdot 7H_2O$, $Ta_6Br_{14}\cdot 7H_2O$, and $Ta_6Cl_{14}\cdot 7H_2O$ are consistent with the assumption of a group M_6X_{12} in which the metal atoms are at the corners of a regular octahedron and the halogen atoms are on the radial perpendicular bisectors of the edges of this octahedron. The shortest interatomic distances in the M_6X_{12} groups are as follows.

Compound	M–M, Å.	M–X, Å.	X···X, Å.
$Nb_6Cl_{14}\cdot 7H_2O$	2.85	2.41	3.37
$Ta_6Br_{14}\cdot 7H_2O$	2.92	2.62	3.64
$Ta_6Cl_{14}\cdot 7H_2O$	2.88	2.44	3.41

These results agree reasonably well with distances calculated on the basis of Pauling's theory of intermetallic distances.

PASADENA, CALIFORNIA RECEIVED JUNE 8, 1950

[CONTRIBUTION FROM THE UNIVERSITY OF COLORADO]

The Near Ultraviolet Absorption Spectra of Some Fluorinated Derivatives of Methane and Ethylene[1,2]

BY J. R. LACHER, L. E. HUMMEL, E. F. BOHMFALK AND J. D. PARK

The ultraviolet absorption spectra of CH_3Cl, CH_3Br and CH_3I show continuous absorption in the long wave length region.[3] Apparently, the absorption of a light quantum brings about the dissociation of the molecule. A possible mechanism is

$$CH_3X + h\nu \longrightarrow CH_3 + X$$

as this will account for the shift in the absorption maximum to the red in the above series of compounds, since the carbon–halogen bond strengths fall off in this order. At shorter wave lengths, discrete bands are obtained which are due to the excitation of non-bonding electrons on a halogen atom.[4] Hukumoto[5] has studied the near ultraviolet absorption spectra of numerous compounds containing halogen, hydroxyl and nitrile groups. The thresholds for the long wave length continuous absorption were used to determine the relative energies of C–X, C–OH and C–CN bonds. The ultraviolet spectra of simple ethylenic hydrocarbons have been thoroughly studied both experimentally and theoretically.[6–9] It was found that the wave length of the first absorption band shifts to the red with increasing number of alkyl groups bound to the carbon atoms of the C=C bond. Price and Tutte[7] correlate this shift with the decrease in heat of hydrogenation of the double bond with increasing alkyl substitution, as has been found by Kistiakowsky and coworkers.[10,11] Since we are in this Laboratory

(1) Presented before the Division of Physical and Inorganic Chemistry, 117th Meeting of the American Chemical Society, Detroit, Michigan, April 16–20, 1950.

(2) This work was supported by Contract N6onr-231, Task Order 6, Office of Naval Research, United States Navy.

(3) G. Herzberg and G. Scheibe, *Z. physik. Chem.*, **7B**, 390 (1930).

(4) W. C. Price, *J. Chem. Phys.*, **4**, 539 (1936).

(5) Y. Hukumoto, *ibid.*, **3**, 164 (1935).

(6) E. P. Carr and H. Stucklen, *ibid.*, **4**, 760 (1936).

(7) W. C. Price and W. T. Tutte, *Proc. Roy. Soc.* (*London*), **174A**, 207 (1940).

(8) R. S. Mulliken, *J. Chem. Phys.*, **7**, 20 (1939).

(9) R. S. Mulliken, *Rev. Mod. Phys.*, **14**, 265 (1942).

(10) G. B. Kistiakowsky, *et al.*, THIS JOURNAL, **57**, 65 (1935).

(11) G. B. Kistiakowsky, *et al.*, *ibid.*, **57**, 876 (1935).